DEPARTMENT OF DEFENCE
DEFENCE SCIENCE & TECHNOLOGY ORGANISATION
DSTO

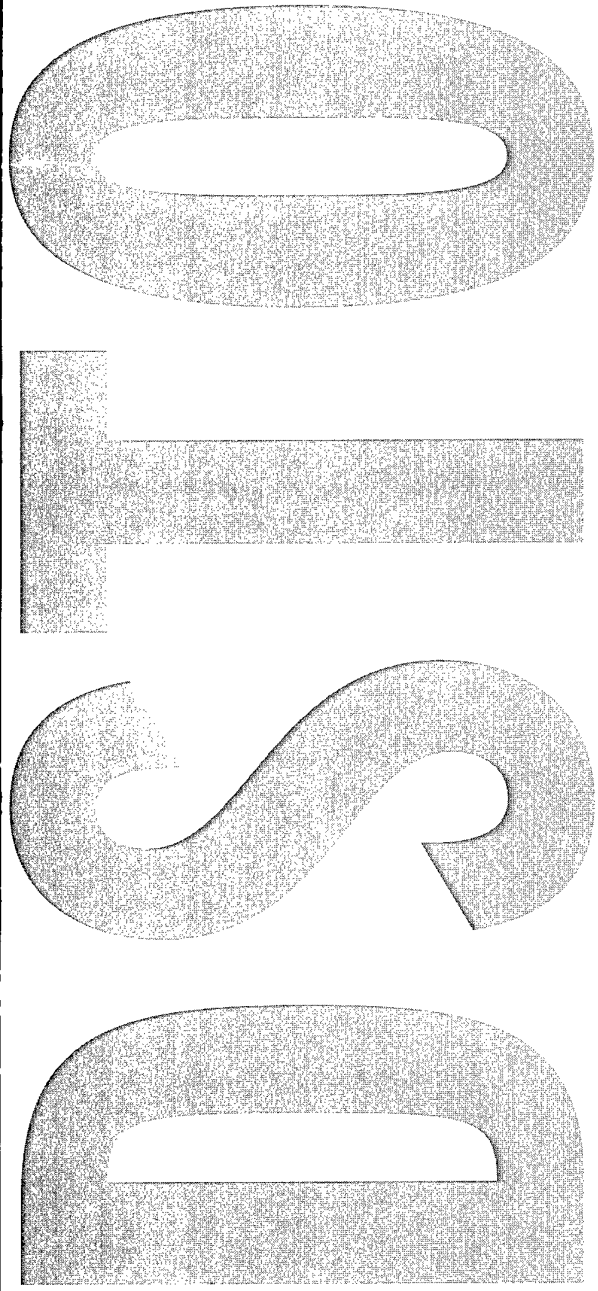

Notch Stress Convergence Studies for H and P Formulation Finite Elements

M. McDonald, M. Heller
and R.J. Wescott

DSTO-TR-1151

Notch Stress Convergence Studies for H and P Formulation Finite Elements

M. McDonald, M. Heller and R.J. Wescott

Airframes and Engines Division
Aeronautical and Maritime Research Laboratory

DSTO-TR-1151

ABSTRACT

In the present investigation both 2D and 3D linear elastic analyses have been undertaken to assess the accuracy and computational resources associated with the use of h-element and p-element formulations. All analyses have been undertaken for a local stress-concentrating feature, which is typical of aircraft structures, namely a circular hole in a remotely loaded plate. Here highly accurate results are obtained for both element formulations, and it is found that the p-elements offer large savings in analysis times. Subsequently a relationship is developed and validated for both 2D and 3D meshes to determine an equivalent non-uniform h-element mesh density, which will yield the same accuracy as a fully converged p-element mesh. This provides a useful transferable tool for designing cost-effective h-element meshes, obviating the need for multiple mesh refinement iterations. Finally, it is demonstrated numerically that p-elements of order five and above, can be used to predict accurate through-thickness peak stresses, in a typical plate modelled with only one element through its full thickness.

DEPARTMENT OF DEFENCE
DEFENCE SCIENCE & TECHNOLOGY ORGANISATION
DSTO

Published by

DSTO Aeronautical and Maritime Research Laboratory
506 Lorimer St
Fishermans Bend Vic 3207 Australia

Telephone: (03) 9626 7000
Fax: (03) 9626 7999

AR-011-864
May 2001

APPROVED FOR PUBLIC RELEASE

Notch Stress Convergence Studies for H and P Formulation Finite Elements

Executive Summary

Finite element methods (FEM) are currently used extensively throughout the Airframes and Engines Division (AED) as part of its role in providing through life support of aircraft in service with the Royal Australian Air Force (RAAF). In particular, stress predictions obtained from FEM are used in designing and validating life extension repairs, assessing the structural integrity of aircraft, and in the life assessment of aging aircraft. Typically, the role of the FE analysis is to determine accurate numerical predictions of peak stresses at local geometric features such as notches, in large and complex components, such as the wing pivot fitting of the F-111 aircraft in service with the RAAF. Historically, the commercial finite element codes used in AED to undertake such stress analyses have used h-element formulations. In recent years p-element formulations have become available in some commercial codes, which potentially offer significant advantages in providing more efficient and cost effective solutions. However, there appears to be limited published results available for 2D and 3D notch stress evaluation using p-elements.

Hence, in the present investigation both 2D and 3D linear elastic analyses have been undertaken to assess the accuracy and computational resources associated with the use of h-element and p-element formulations. All analyses have been undertaken for a local stress-concentrating feature, which is typical of aircraft structures, namely a circular hole in a remotely loaded plate. Here highly accurate results are obtained for both element formulations, and it is found that the p-elements offer large savings in analysis times. Subsequently a relationship is developed and validated for both 2D and 3D meshes to determine an equivalent non-uniform h-element mesh density, which will yield the same accuracy as a fully converged p-element mesh. This provides a useful transferable tool for designing cost-effective h-element meshes, obviating the need for multiple mesh refinement iterations. Finally, it is demonstrated numerically that p-elements of order five and above, can be used to predict accurate through-thickness peak stresses, in a typical plate modelled with only one element through its full thickness.

The results obtained in the present work provide valuable transferable outputs, which can be used to undertake cost effective analyses for both h-element, and p-element technologies, relating to the structural assessment of RAAF aircraft. It is noteworthy that very recently these results have been used for efficient FE analysis of large-scale structural models, as part of the Australian F-111 Aircraft Structural Integrity Sole Operator Program.

Authors

M. McDonald
Airframes and Engines Division

Marcus McDonald completed a Bachelor of Engineering. (Hons Mechanical) at the University of Queensland in 1994. Prior to joining AMRL in 1998 he spent 3 years working in the oil & gas, steel and railway industries using finite element methods for structural design projects and failure investigations. Since joining AMRL he has applied his broad knowledge of finite element stress analysis to the areas of structural integrity and life extension of Australian Defence Force aircraft. He is currently a Professional Officer in the Airframes and Engines Division.

M. Heller
Airframes and Engines Division

Manfred Heller completed a B. Eng. (Hons.) in Aeronautical Engineering at the University of New South Wales in 1981. He commenced employment in Structures Division at the Aeronautical Research Laboratory in 1982. He was awarded a Department of Defence Postgraduate Cadetship in 1986, completing a PhD at Melbourne University in 1989. He is currently a Principal Research Scientist and Functional Head for Structural Mechanics in the Airframes and Engines Division. His research contributions have focused on the areas of stress analysis, structural shape optimisation, and bonded repair technology, in the context of airframe life extension. Since 1992 he has led tasks, which develop and evaluate techniques for extending the fatigue life of ADF aircraft components. He is a Corresponding Member, Committee on Stress Analysis and Strength of Components, Engineering Science Data Units (ESDU) UK.

R.J. Wescott
Airframes and Engines Division

Ron Wescott graduated from the University of Melbourne in 1973 as a B. Eng (Civil) with First Class Honours. In 1981 he was awarded a Ph.D from the same university, where his research work involved the development of a finite element method for the geometrically and materially nonlinear analysis of rigid-jointed frames, and included the capability to predict response after the peak load is reached. He spent more than ten years in industry developing, maintaining and using computer-aided engineering and mining systems. He has had five years experience in the automotive industry using commercial finite element packages to aid the design of car seat components. His services are gained through Aerostructures Technologies.

Contents

1. Introduction

Finite element methods (FEM) are currently used extensively throughout the Airframes and Engines Division (AED) as part of its role in providing through life support of aircraft in service with the Royal Australian Air Force (RAAF). In particular, stress predictions obtained from FEM are used in designing and validating life extension repairs, for assessing the structural integrity of aircraft, and in the life assessment of ageing aircraft. Typically, the role of the FE analysis is to determine accurate numerical predictions of peak stresses at local geometric features such as notches in large and complex components, such as the wing pivot fitting of the F-111 aircraft in service with the RAAF. Historically, the commercial finite element codes used in AED to undertake most of the stress analyses have used h-formulation elements[1]. In recent years, p-formulation elements[1] have become available in some codes, which potentially offer significant advantages in providing more efficient and cost effective solutions.

In the FEM of computational stress analysis, a component is modelled as an assemblage of discrete (or finite) elements. If conventional h-element FE technology is adopted [1], the analysis error in predicted peak stresses generally decreases as the size of elements decreases. This is because typically each element can accurately model a linear variation in stress, however throughout the structure the stress distribution is significantly non-linear. Hence to obtain accurate stress results, a modeller would ideally perform several analyses of the same geometric model using an increasing number of smaller elements, until convergence was achieved (i.e. stopping when the peak stress difference between successive analyses falls to an acceptable level). One difficulty with this approach is that a new geometric element mesh must be created for each successive analysis. Remeshing can be a highly time consuming task for the modeller, even if state-of-the-art pre-processing tools are used (particularly for models which have cracks or are three-dimensional). Also, progressively greater computational resources are then needed in the solution phase.

Unlike h-elements, p-elements are defined by variable order polynomial displacement functions, and hence can potentially model higher order stress variations in each element accurately. Here to achieve convergence, instead of reducing the element size, only the polynomial order of the elements needs to be increased. However, while p-elements have been reported in the literature for several years [2-5], it appears that comparisons of the relative performance of p-elements and h-elements have only been made for some limited two-dimensional (2D) problems [6]. Also, there appear to be limited publications relating to the use of p-elements for more complex applications, and only in recent years have p-elements become available to some extent in commercial FE codes. For instance, p-elements are available in MSC.NASTRAN [7] for linear elastic analysis, but not for plasticity analysis, and ABAQUS [8] and PAFEC [9] do not have p-elements at all. Hence, before the p-element approach can be used with

[1] For brevity, h-formulation elements will be referred to as h-elements and p-formulation elements as p-elements in the rest of the report.

confidence in AED, it is considered beneficial to undertake some appropriate benchmark studies comparing the performance of the two element types for the calculation of typical notch stresses, in two and three dimensions. Also of further interest is the hypothesis that even if a FE code does not support p-element technology, an alternate p-element analysis in another code may be useful in guiding the design of an equivalent h-element mesh, without the need for time consuming multiple mesh refinement iterations.

Hence in the present investigation, both 2D and 3D analyses were undertaken to assess the accuracy and computational resources needed for various uniformly distributed h-element and p-element mesh densities, and p-element orders. All analyses are undertaken for a local stress-concentrating feature, which is typical of aircraft structures, namely a circular hole in a remotely loaded plate. From these results, an empirical relationship is then developed for both 2D and 3D meshes to determine, in one iteration, the non-uniform h-element mesh density which will yield approximately the same accuracy as a given non-uniform order p-element mesh. Through a numerical example, the veracity of this approach is then investigated as a potential transferable tool in designing cost-effective h-element meshes. Finally, an investigation is undertaken to determine the p-element modelling requirements for the accurate and efficient prediction of peak (and non-uniform) through-thickness stresses in plates.

2. Geometry and Finite Element Approach

Circular holes in loaded plates are a common stress-concentrating feature of aircraft structures, and hence this is the case that has been chosen for the present numerical benchmark analyses. The geometry under consideration is shown in Figure 1. Here the flat plate contains a centrally located hole of radius r and is loaded by a uniaxial remote stress S_1, on the faces at $x = \pm 10.177r$, in the x direction. The plate width is 8.496r while the thickness is $1.77r$. This specific plate geometry has been chosen to allow convenient comparison with prior published 3D FE results [10]. In the present work one plane of symmetry was invoked for all 2D analyses, while typically three planes of symmetry were utilised for the 3D analyses. For all analyses the hole radius was taken as $r = 11.3$ mm and remote stress was $S_1 = 30$ MPa. Also, the numerical values for the material constants were chosen to be representative of an aluminium alloy, with Young's Modulus taken as 73049 MPa, and Poisson's ratio taken as 0.33.

All analyses were undertaken using a Hewlett-Packard K Series 9000 computer located in AED. The finite element codes PAFEC (Version 8.5) and MSC.NASTRAN (Version 69) were used for the h-element runs, and the p-element runs were performed in MSC.NASTRAN (Versions 69 and 70.5). Pre-processing and post-processing for the PAFEC and MSC.NASTRAN analyses were undertaken using PIGS and MSC.PATRAN (Versions 7.0A and 7.5) respectively.

For the p-element analyses it was important to remove all possible sources of singularity for this study, because very accurate results were required. Hence typically the following techniques were adopted in the modelling process: (i) loads were applied as pressures on element edges (2D cases) or faces (3D cases) rather than as forces on nodes, and similarly (ii) constraints were applied to element edges or faces rather than to nodes. Also, all element edges are considered to be straight unless specified otherwise. It is noted that when using MSC.NASTRAN, to obtain highly accurate results, the shape of curved external edges must be specified precisely. Hence for the analyses presented in Sections 3 and 4 the edges were defined by equations representing a circular arc. This method required manual insertion of equations and element edge definitions into the MSC.NASTRAN input deck. However, based on the work in Sections 3 and 4, it was concluded that this approach would be too time consuming for the modelling of complex structures. Hence, the final set of 3D analyses (see Section 5) was performed with 32-noded brick elements, which have two midside nodes on each element edge [7]. These midside nodes were used to implement the two-point method for defining the curvature of curved element edges and faces in MSC.NASTRAN.

An error measure for predicted K_t was used to assess the accuracy of the various modelling techniques and mesh densities. In this study the error was defined as:

$$\varepsilon_{Kt} = (K_{t(FEA)} - K_{t(exact)}) / K_{t(exact)} \quad (1)$$

where $K_{t(FEA)}$ is the maximum stress concentration factor from the analysis under consideration, and $K_{t(exact)}$ is the exact solution for maximum stress concentration factor. The present geometry is a finite width plate, for which no closed form theoretical solution appears to be available, although an approximate solution obtained by Howland gives a value of $K_t = 3.21$ [11]. Hence in the present work, the 'exact' solution is taken to be the result from the most converged analysis, which, for both the 2D and 3D benchmarks, was obtained from a high order p-element analysis.

3. Convergence of 2D P-Element and H-Element Benchmarks

3.1 Convergence Analyses

In this section benchmark results are given for several variations of 2D p-element and h-element meshes. In these plane-stress analyses the plate thickness was arbitrarily selected as 10 mm. MSC.NASTRAN was used for the p-element runs and PAFEC for the h-element analyses, with the aim of comparing the accuracy and efficiency of the two element formulations. In all analyses the element mesh density was approximately uniform. The PAFEC h-element analyses used 8-noded iso-parametric quadrilateral elements, whereas 4-noded quadrilateral p-elements (which can have curved edges)

were used in the MSC.NASTRAN analyses. For the PAFEC h-element analyses, the mesh density was varied from one division per half-width of the plate to 32 divisions per half-width, as shown in Figure 2. Hence, the number of h-elements varied from 10 to 10240. The base model for the MSC.NASTRAN p-element analyses contained 40 elements as shown in Figure 2(b), i.e. the same mesh as the PAFEC h-element analysis with two divisions per half-width. Seven p-element analyses were conducted with the polynomial order of the elements taking values from one to seven [12], with all elements having the same polynomial order in an individual analysis.

3.2 Convergence Results

For all analyses, results for the following were obtained: (i) number of degrees of freedom[2], (ii) total analysis time, (iii) maximum stress concentration factor, and (iv) percent error in the maximum stress concentration factor. These results are listed in Tables 1 and 2 for the h-element and p-element analyses respectively. Table 2 also gives results obtained from the MSC.NASTRAN error estimator at the grid point (i.e. node) location with the maximum stress concentration factor. The MSC.NASTRAN grid point error estimator [7] is based on the differences in stress computed from all elements that use the designated grid point (i.e. grid point stress discontinuity). Because a converged or 'exact' value of maximum stress concentration factor is available, it is possible to assess the accuracy of the MSC.NASTRAN error estimator for p-elements. As expected, it was found that the maximum stress concentration always occurred at the location $x = 0$, $y = r$. It is interesting to consider the behaviour of total analysis times as a function of the number of degrees of freedom (DOFs). This behaviour is plotted in Figure 3 using a log-log scale. While the responses are different, it is seen that analysis times are roughly the same for p-elements and h-elements for the same numbers of degrees of freedom. The differences in analysis times are further discussed in Section 4.2 for 3D analyses.

Table 1: PAFEC results for 2D h-element analyses.

No. elements	No. DOFs	Total analysis time (seconds)	Maximum stress concentration factor	Error (ε_{Kt})
10	77	1	2.67700	-16.80%
40	275	2	3.19310	-0.76%
160	1031	6	3.26483	1.47%
640	3983	24	3.24225	0.77%
2560	15647	142	3.22587	0.26%
10240	62015	1173	3.21923	0.05%

[2] MSC.NASTRAN outputs an equivalent number of active DOFs for p-element analyses.

Table 2: MSC.NASTRAN results for 2D p-element analyses.

P-element order	No. DOFs	Total analysis time (seconds)	Maximum stress concentration factor	Error (ε_{Kt})	MSC.NASTRAN error estimate
1	588	5.6	2.93351	-8.83%	6.10%
2	744	5.6	3.28906	2.22%	10.05%
3	1356	6.6	3.23722	0.61%	1.05%
4	2608	9.6	3.22598	0.26%	0.62%
5	3660	14.6	3.21738	-0.006%	0.09%
6	4912	25.4	3.21742	-0.004%	0.04%
7	6364	40.2	3.21756($K_{t(exact)}$)	0%	0.03%

It can be seen that there was very good agreement in the final converged values of stress concentration factor for both element types. Here the h-element analyses converged to a maximum stress concentration factor of 3.21923 with the difference between the last two analyses being 0.206%. Here, as indicated in Table 1, the mesh density was increased until the convergence behaviour was monotonic for 3 successive analyses. The p-element analyses converged to a maximum stress concentration factor of 3.21756, with the difference between the last two analyses (orders six and seven) being only 0.004%[3]. Hence for the p-element analyses, the convergence behaviour can be considered as being very good, with only small oscillation about the final converged value as the element order was increased. This is important to note since it indicates good robustness in the approach.

Figure 4 shows the relationship between the absolute value of the percentage error and the number degrees of freedom for both h-element and p-element cases, plotted on a log-log scale. The lines of best fit indicate that the rate of convergence (or decrease in error) is significantly faster for p-elements. The results in Table 2 also show that the MSC.NASTRAN error estimator gives a useful and conservative estimate of the 'true' error, for all 2D p-element orders greater than one.

3.3 Empirical 2D 'P-Element Order' and 'H-Element Mesh Density' Relationship

Here a relationship is sought between the order of a 2D p-element model and the mesh density of an h-element model with the same mesh discretization error, based on the results given in the preceding section, for an approximately uniform mesh density.

[3] Based on the discussion in Section 2, the 'exact' solution for the 2D analyses is taken as $K_{t(exact)} = 3.21756$.

This is sought on the basis that the relationship may be applicable to specifying a high quality non-uniform h-element mesh (in one iteration) based on the results of an automated p-element convergence study. For example an accurate, high order p-element analysis using a relatively course geometric mesh in MSC.NASTRAN may be used to guide the design of a high quality h-element mesh in ABAQUS (which does not support p-elements), without the need for time consuming multiple geometric mesh refinement iterations.

First we can postulate that the negative log of the error is a linear function of p-element order. Figure 5 represents the data in this form, where the fitted equation is also given[4]. The correlation coefficient (R^2) is 0.9453, which indicates that the fit of the data to the hypothesised relationship is very good. Next for h-elements, it is hypothesised that the negative log of the error has a power dependence on the number of h-element divisions. Figure 6 shows the line of best power fit and the equation of that line. In this case, the correlation coefficient (R^2) is 0.7419. The poorer correlation is due to the greater oscillation of results for low numbers of h-element divisions. We can now equate the response equations given in Figure 5 and Figure 6 to obtain:

$$h = (0.5112p + 0.1586)^{3.0469} \tag{2}$$

where p is the order of the p-element and h is the number of h-element divisions per p-element division. Equation (2) is represented graphically in Figure 7.

It is important to note that this equation is based on FE results for models with approximately uniform h-element mesh densities, and/or uniform p-element order distributions. Potential applicability to non-uniform cases is discussed subsequently.

3.4 Trial of H-P Element Density Relationship for Non-Uniform Meshes

In this section the empirical relationship obtained in the previous section, based on approximately uniformly distributed mesh density (i.e. h-element size or p-element order), is assessed for the case where the mesh density is significantly non-uniform. For this trial the base p-element FE model had 40 elements, and is shown in Figure 2(b). The steps used to conduct the trial were as follows; (i) analyse the base p-element model with the auto-order option, (ii) apply the h-p relationship from Equation (2) to create an equivalent h-element model using the auto-order results, and (iii) analyse the h-element model, and compare the error from the p-element and h-element models.

The auto-order p-element analysis starting p-order was set at one, and the maximum allowed p-order was five. The iterative analysis was terminated when the maximum node stress discontinuity, from adjacent elements, became less than one per cent.

[4] Microsoft Excel 97 SR-1 was used to determine the line of best fit.

Figure 8 shows the final p-element orders for each element, from the MSC.NASTRAN analysis, which range from two to five. Table 3 shows the number of edge divisions (rounded to the nearest integer) used in the equivalent h-element model as a function of the p-element order. If elements sharing a common edge had different orders, the higher order was used to divide the edge. Figure 9 shows the resulting h-element model, which contained 6492 elements. It is noteworthy that Figure 9 indicates that the maximum density of h-elements radiates from the 45-degree positions where the shear stresses are the greatest. This confirms that typically for an approximately uniform distribution of h-element sizes, FE errors are greatest where element shear stresses are highest. This feature appears not to be well known, as some analysts incorrectly assume that the greatest mesh density should be at the location of peak direct stress.

Table 3: H-element edge divisions (to nearest integer) equivalent to p-element order.

P-element order	Equivalent h-element edge divisions
2	2
3	5
4	11
5	21

Results of the two analyses are compared using the error measure defined in Section 2, where $K_{t(exact)}$ is given in Section 3.2. The p-element analysis gave an error in K_t of 0.555%, whereas the h-element analysis error was 0.087%. Hence the empirical relationship has been very useful, providing a conservative h-element analysis result, which has less error than the initial accurate p-element analysis. If it is desired to reduce the level of conservatism it may be useful to use the average of the two element orders to divide the shared edge, as opposed to using the higher p-element order.

Hence in summary, the results obtained in this section indicate that assuming a 2D p-element analysis with automatic ordering has been performed, the resultant element orders, in conjunction with equation (2), can guide the modeller in efficiently designing a h-element mesh for further complex analysis for which p-element technology is not available.

4. Convergence of 3D P-Element and H-Element Benchmarks

4.1 Convergence Analyses

This section reports on analyses with several variations of 3D p-element and h-element meshes. The following specific element cases were analysed, (i) MSC.NASTRAN 8-noded brick p-elements, (ii) MSC.NASTRAN 8-noded brick h-elements, (iii) MSC.NASTRAN 20-noded iso-parametric brick h-elements, and (iv) PAFEC 20-noded iso-parametric brick h-elements. A model composed of 20 elements, as shown in Figure 10 (a), was the starting point for all sets of h-element analyses. In the case of the MSC.NASTRAN 8-noded and 20-noded brick h-elements, the mesh density was uniformly varied in three dimensions from one element through the half thickness of the plate to eight elements through the half thickness. Typical meshes are shown in Figure 10 (a-c). Similarly, for the PAFEC 20-noded brick h-elements, the mesh density was varied from one to six elements through the plate half thickness. The model for the p-element analyses was the same as the base model for the h-element analyses, with the polynomial order of the elements varying from one through to eight.

4.2 Convergence Results

The key output results obtained for the various analysis cases are given in Table 4 to Table 7, as a function of mesh size or element order. Here to determine the error, the exact value was taken as $K_{t(exact)} = 3.3754$ (from Table 10, Section 5.2).

Table 4: MSC.NASTRAN results for 8-noded brick p-element analyses.

P-element order	No. DOFs	Total analysis time (seconds)	Maximum stress concentration factor	Error (ε_{Kt})
1	351	4.8	3.1494	-6.70%
2	462	5.3	3.4975	3.62%
3	1053	7.0	3.4413	1.95%
4	2684	12.9	3.3983	0.68%
5	3895	30.0	3.3867	0.34%
6	5346	50.6	3.3739	-0.04%
7	7217	114.8	3.3775	0.06%
8	9568	267.8	3.3762	0.02%

Table 5: MSC.NASTRAN results for 8-noded brick h-element analyses.

No. elements	No. DOFs	Total analysis time (seconds)	Maximum stress concentration factor	Error(ε_{Kt})
20	131	3.4	2.6863	-20.42%
160	742	5.4	3.1533	-6.58%
540	2193	11.1	3.3084	-1.98%
1280	4844	21.7	3.3651	-0.30%
2500	9055	41.6	3.3901	0.43%
4320	15186	77.2	3.4015	0.77%
6860	23597	139.9	3.4072	0.94%
10240	34648	224.3	3.4097	1.02%

Table 6: MSC.NASTRAN results for 20-noded brick h-element analyses.

No. elements	No. DOFs	Total analysis time (seconds)	Maximum stress concentration factor	Error(ε_{Kt})
20	442	4.2	3.4646	2.64%
160	2684	12.7	3.5352	4.74%
540	8166	38.5	3.4792	3.07%
1280	18328	98.6	3.4463	2.10%
2500	34610	226.6	3.4265	1.52%
4320	58452	627.8	3.4144	1.15%
6860	91294	N.A[5]	3.4044	0.86%
10240	134576	N.A	3.3980	0.67%

[5] The final two analyses were run on a different hardware platform, and hence the total analysis times cannot be validly compared with other results.

Table 7: PAFEC results for 20-noded brick h-element analyses.

No. elements	No. DOFs	Total analysis time (seconds)	Maximum stress concentration factor	Error(ε_{Kt})
20	442	3.8	3.4187	1.28%
160	2684	30.3	3.5212	4.32%
540	8166	173.2	3.4603	2.52%
1280	18328	992.5	3.4330	1.71%
2500	34610	4052.8	3.4166	1.22%
4320	58452	13239.4	3.4062	0.91%

The results in Table 5 and Table 6 show that the MSC.NASTRAN h-element analyses with 8-noded bricks required about the same analysis time per degree of freedom as compared to the MSC.NASTRAN h-element analyses with 20-noded bricks. Comparison of Table 6 and Table 7 shows that unlike the 2D cases, the 3D PAFEC analysis times for h-elements was about an order of magnitude greater than for the MSC.NASTRAN h-element analysis times for the larger models. Although the PAFEC time includes time for mesh generation (unlike MSC.NASTRAN), it is believed that most of the increase is due to other differences between the two codes and/or how the specific features of the codes interact with computer system configuration. Table 4 shows that the times per degree of freedom for the p-element analyses were similar to the MSC.NASTRAN h-element runs for lower element orders (one to four), but were greater for higher element orders (five to eight). However, one key point from Tables 4 and 6, is that the total solution time for a uniform order p-element analysis is much less than that for uniform density h-element anaysis, for a typical error of 1%.

For convenience the maximum stress concentration factor results in Table 4 to Table 7 are summarised in Figure 11. It is interesting to note that for all element types there is good agreement in K_t to within 1% error. Here it appears all cases are converging monotonically to the true K_t result, except the MSC.NASTRAN 8-noded brick h-elements, which are converging to a result approximately 1% higher than the true value. As expected the p-element analyses showed the highest degree of convergence, reaching to within 0.06 percent and 0.02 percent of the exact solution with p-elements of order seven and eight respectively, and with the least degrees of freedom.

Figure 12 gives the response of the absolute value of the percentage error as a function of the number of degrees of freedom, for the four sets of analyses. As expected it can be seen that the p-element method is efficient and accurate since it requires significantly less analysis time to achieve a solution within one percent of the 'exact' solution. By contrast, both 20-noded brick methods require large numbers of degrees of freedom and analysis times.

4.3 Empirical 3D 'P-Element Order' and 'H-Element Mesh Density' Relationship

In this section an empirical relationship is derived between the order of a 3D p-element model with uniform order distribution, and the uniform mesh density of an h-element model (20-noded brick) with the same mesh discretization error. Here a similar method was used as described for the 2D case in Section 3.3. Initially it is hypothesised that the negative log of the error is a linear function of p-element order, where Figure 13 represents the data in this form. Here the line of best linear fit[6] is given, which has a correlation coefficient (R^2) of 0.9635. For the 20-noded h-elements, it is hypothesised that the negative log of the error has a linear dependence on the log of the number of h-element divisions. Using this assumption, Figure 14 shows the lines of best fit for both the MSC.NASTRAN and PAFEC cases, where the correlation coefficients (R^2) are 0.9891 and 0.9986 respectively[7]. The three correlation coefficients all indicate a very good fit of the data to the hypothesised relationships. Hence combining the fitting equations given in Figure 13 and Figure 14 results in:

$$h = e^{(0.6076p - 0.2267)} \tag{3}$$

for MSC.NASTRAN h-elements, and

$$h = e^{(0.6096p - 0.3491)} \tag{4}$$

for PAFEC h-elements, where p is the order of the p-element and h is the number of h-element divisions per p-element division. Equation (3) and Equation (4) are represented graphically in Figure 15. It is noted that comparison of Figure 7 and Figure 15 shows that the h-p element 2D and 3D relationships yield about the same values for h-element mesh density for a given p-element order.

It is important to note that the above empirical 3D relationship has been trailed in a practical application involving notch stress evaluation in a large-scale FE model of the F-111 wing pivot fitting. In that work the local h-element mesh, around critical fuel flow vent holes, was designed so that a non-linear analysis could be performed using ABAQUS, by undertaking an initial p-element analysis of a relatively coarse mesh in MSC.NASTRAN. This proved to be useful in providing accurate complex h-element mesh with minimal iterations [13]. Here it should be noted that p-elements are currently not available for non-linear use, in any commercial code.

---

[6] Microsoft Excel 97 SR-1 was used to determine the line of best fit.

[7] Results for both MSC.NASTRAN and PAFEC analyses with one h-element division do not follow the trend, and hence are excluded from curve fitting.

5. P-Element Modelling of Through Thickness Stresses

5.1 Analysis

In this section further work is reported which focuses solely on several variations of 3D p-element analyses. Here the aim is to investigate in detail the accuracy of different combinations of mesh densities and element orders for determining the peak stress distribution through the thickness of a plate, at the hole boundary. In particular, to determine whether the known non-uniform through thickness variation in K_t can be accurately modelled with a single element. As indicated in Section 2, here 32-noded brick p-elements were used, so that two midside nodes could be used to define the curvature of elements around the hole perimeter. Table 8 summarises the four p-element FE geometric models used in this investigation, and Figure 16 shows the corresponding FE meshes. It should be noted that the first listed mesh was a full plate thickness model while the other three were half thickness models. The results obtained are to be subsequently compared to results from an accurate PAFEC analysis with a highly refined non-uniform h-element mesh [10]. For reference, the local detail of the mesh for the PAFEC analysis is shown in Figure 17. For each of the present analyses, the p-element order (uniform throughout the mesh) was increased by one until the change in the maximum stress concentration factors between successive analyses was less than 0.05%.

Table 8: P-element FE modelling for through thickness stress analysis.

Total no. of elements in model	Equivalent no. of elements through full thickness	Symmetry used
20	1	2 planes
20	2	3 planes
160	4	3 planes
1280	8	3 planes

5.2 Results and Discussion

The maximum stress concentration factor results at various locations through the plate thickness are given for each of the four meshes as a function of p-element order in Figures 18 to 24. These are sequenced as follows: (i) one element through the full plate thickness in Figures 18 and 19, (ii) two elements through the full plate thickness in Figures 20 and 21, (iii) four elements through the full plate thickness in Figures 22 and 23, and (iv) eight elements through the full plate thickness in Figure 24. In each of the

four mesh cases, very good converged stress results were achieved as the p-element order was increased. As can be expected, more pronounced oscillation about the exact stress distribution occurs for low p-element orders for the least refined mesh, as shown in Figure 18. Conversely, for the more refined meshes, there is minimal oscillation even for low p-element orders, as evidenced in Figure 24. To allow more precise comparison, the convergence results as a function of p-element order are given in Table 9, where the difference in the maximum stress concentration factors between successive analyses was less than 0.05%. It can be seen that the four p-element models converged to maximum stress concentration factors in the range 3.3754 to 3.3756[8]. This compared to a maximum stress concentration factor of 3.3790 from the PAFEC analysis with the highly refined non-uniform h-element mesh [10]. Similarly, Table 10 shows the p-element order required for each model to obtain accurate (but less stringent) results to better than 0.5% error.

Table 9: P-element order required for converged results better than 0.05% difference between successive iterations for different element meshes.

Equivalent no. of elements through full thickness	P-element order	Converged maximum stress Concentration factor
1	8	3.3756
2	8	3.3756
4	6	3.3754
8	5	3.3755

Table 10: P-element orders required for accurate results with error less than 0.5% for different element meshes.

Equivalent no. of elements through full thickness	P-element order	Error(ε_{Kt})	MSC.NASTRAN error estimate
1	5	0.30%	0.014%
2	5	-0.33%	0.0033%
4	4	-0.11%	0.00061%
8	3	-0.15%	0.026%

[8] The smallest difference between consecutive results occurred for four elements through the plate thickness with p-element orders 5 and 6. Hence 3.3754 is considered to be the 'exact' solution for analyses with 3D (brick) p-elements.

An assessment can also be made of the accuracy of the MSC.NASTRAN grid point error estimator[9] for 3D p-elements. From Table 10 it can be seen that unlike the 2D analysis results, the 3D MSC.NASTRAN error estimator underestimates the true error for these higher orders. However, it is worth noting that in almost all cases with p-element order greater than two, the error in maximum stress concentration factor is less than one percent.

In summary, an important result is that unlike h-elements, p-elements (of order five and above) can be used for the present loading to predict accurate through-thickness peak stresses in plates modelled with only one element through the full plate thickness. Based on the present results, this feature has been used in some recent large-scale FE of RAAF airframe components, to save significant resources in FE mesh generation time, and numerical computation [13-17].

6. Conclusion

For a typical local stress concentrating structural feature, namely a circular hole in a remotely loaded plate, both 2D and 3D analyses have been undertaken to assess the accuracy and computational resources needed for various uniformly distributed h-element and p-element mesh densities, and p-element orders. Very accurate converged results were obtained for both element formulations. However, as expected, p-elements offered large reductions in analysis times. Using these results, an empirical relationship was developed for both 2D and 3D meshes to determine the equivalent non-uniform h-element mesh density which will yield approximately the same accuracy as a given non-uniform order and converged p-element mesh. Through a numerical example, the veracity of this approach was confirmed, and hence this approach provides a valuable transferable tool in designing cost-effective h-element meshes, obviating the need for multiple mesh refinement iterations. This is particularly important for large-scale finite element modelling where p-element technology is not available currently, such as the ABAQUS and PAFEC codes, which are used in AED for non-linear analysis and automated shape optimisation respectively. Finally, an investigation was undertaken which demonstrated that p-elements of order five and above can be used to predict accurate peak through-thickness stresses in plates modelled with only one element through the wall thickness.

[9] The MSC.NASTRAN error estimator is described in Section 3.2.

7. References

1. **ZIENKIEWICZ, O.C.,** *The Finite Element Method in Engineering Science,* McGraw-Hill, 1971.
2. **PEANO, A.G.,** *Hierarchics of Conforming Finite Elements for Elasticity and Plate Bending,* Computational Mathematics and Application, 2, 3-4, 1976.
3. **ZIENKIEWICZ, O.C., GAGO, J.P.DeS.R. and KELLY, D.W.,** *The Hierarchical Concept in Finite Element Analysis,* Computers and Structures, 16, 53-65, 1983.
4. **ZIENKIEWICZ, O.C. and ZHU, J.Z.,** *A Simple Error Estimator and Adaptive Procedure for Practical Engineering Analysis,* International Journal for Numerical Methods in Engineering, 24, 337-357, 1987.
5. **BATHE, K.J., LEE, N. and BUCALEM, M.L.,** *On the Use of Hierarchical Models in Engineering Analysis,* Computer Methods in Applied Mechanics and Engineering, 82, 5-26, 1990.
6. **BABUSKA, I. and SZABO, B.,** *On the Rates of Convergence of the Finite Element Method,* International Journal for Numerical Methods in Engineering, 18, 323-341, 1982.
7. **MACNEAL-SCHWENDLER CORPORATION,** 815 Colorado Boulevard, Los Angeles, CA 90041-1777, *MSC.NASTRAN Linear Statics Analysis User's Guide, V69+.*
8. **HIBBITT, KARLSSON & SORENSEN, INC.,** 1080 Main Street, Pawtucket, RI 02860-4847, *ABAQUS/Standard User's Manual, Version 5.8.*
9. **SER SYSTEMS LTD,** 39 Nottingham Rd, Stapleford, Nottingham NG9 8AD, *PAFEC-FE Level 8.0 Data Preparation Manual.*
10. **EVANS, R.L.,** *Effect of Plate Thickness on the In-Plane and Through-Thickness Stresses at a Hole,* Technical Report, TR-0330, Aeronautical and Maritime Research laboratory, Melbourne, Australia, 1996.
11. **HOWLAND, R. C. J.,** *On the Stresses in the Neighbourhood of a circular hole in a strip under Tension,* Iphil. Trams. Roy. Soc. (London), A 229, p67, 1929-1930.
12. **MACNEAL-SCHWENDLER CORPORATION,** 815 Colorado Boulevard, Los Angeles, CA 90041-1777, *MSC.NASTRAN Reference Manual, V68.*
13. **McDONALD, M., MAAN, N., and MORAS, F.,** *Validation and Enhancement of the F-111 Wing Pivot Fitting NASTRAN Model,* Technical Report in preparation, File M1/9/846, Aeronautical and Maritime Research Laboratory, Melbourne, Australia, 2001.
14. **WELLER, S., and McDONALD, M.,** *Stress Analysis of the F-111 Wing Pivot Fitting,* DSTO-TN-0271, Aeronautical and Maritime Research Laboratory, Melbourne, Australia, 2000.

15. **HELLER, M., McDONALD, M., BURCHILL, M., and WATTERS, K.C.,** *Shape Optimisation of Critical Stiffener Runouts in the F-111 Wing Pivot Fitting,* DSTO-TR-1119, Aeronautical and Maritime Research Laboratory, Melbourne, Australia, 2001.

16. **HELLER, M., BURCHILL, M., McDONALD, M., and WATTERS, K.C.,** *Shape Optimisation of Critical Fuel Flow Vent Holes in the F-111 Wing Pivot Fitting,* DSTO-TR-1120, Aeronautical and Maritime Research Laboratory, Melbourne, Australia, 2001.

17. **McDONALD, M., HELLER, M., GOLDSTRAW, M., and HEW, A.,** *Robustness of the F-111 Wing Pivot Fitting Optimal Rework Shapes,* DSTO-TR-1121, Aeronautical and Maritime Research Laboratory, Melbourne, Australia, 2001.

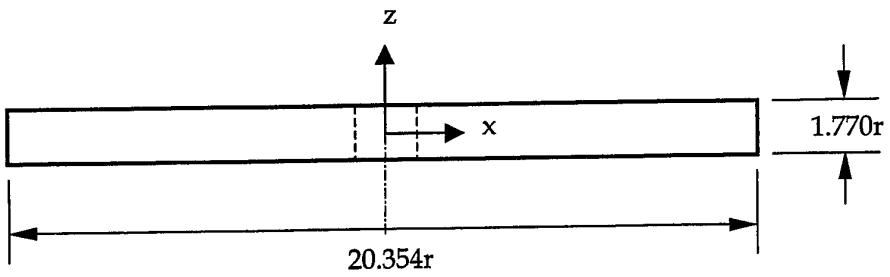

(a) side view

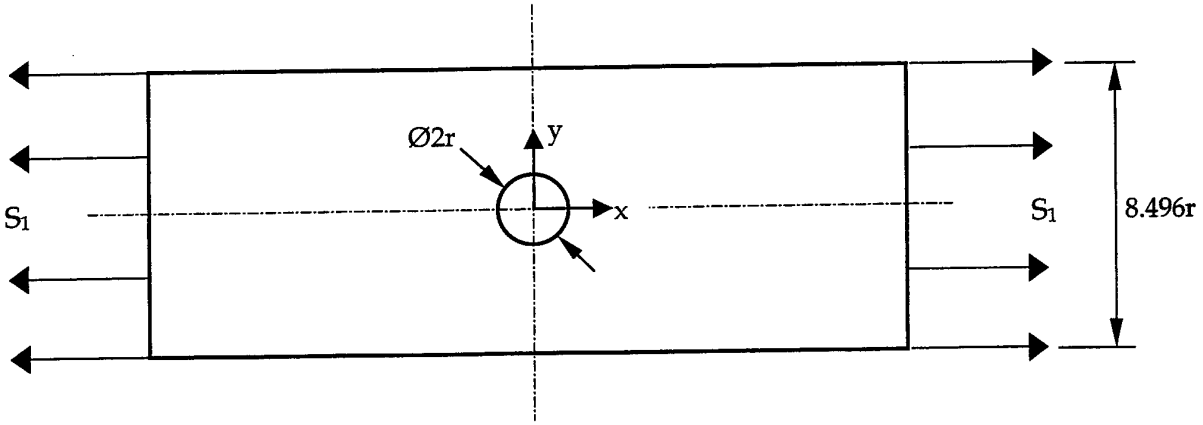

(b) top view

Figure 1: Geometry and loading for plate specimen with circular hole.

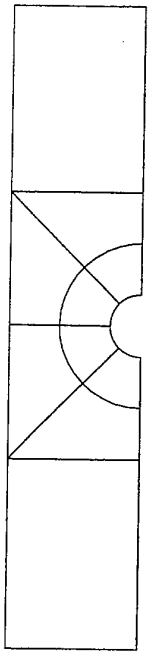

(a) One division

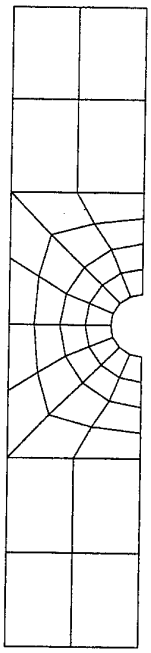

(b) Two divisions

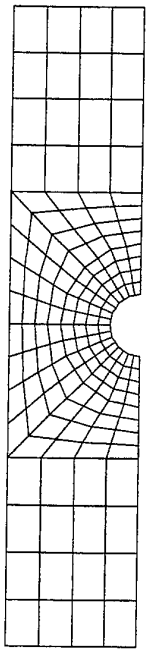

(c) Four divisions

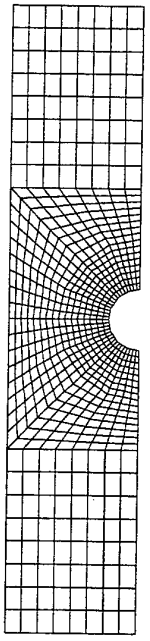

(d) Eight divisions

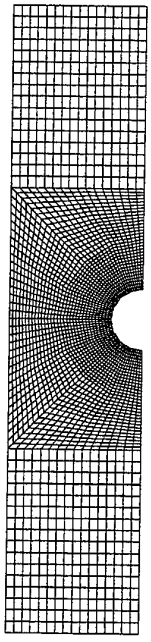

(e) Sixteen divisions

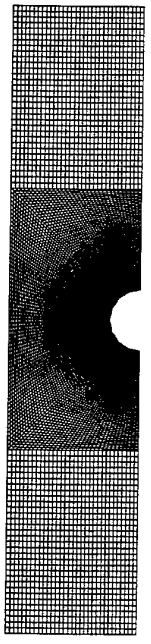

(f) Thirty-two divisions

Figure 2: Two-dimensional finite element meshes for h-element analysis, indicating number of divisions per half width of plate specimen.

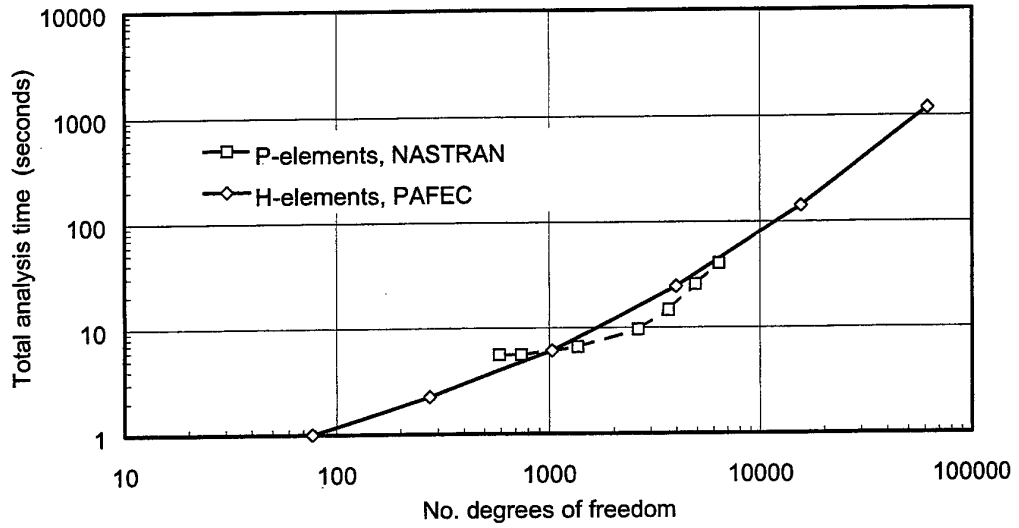

Figure 3: Relationship between analysis time and degrees of freedom for 2D h- and p-element models.

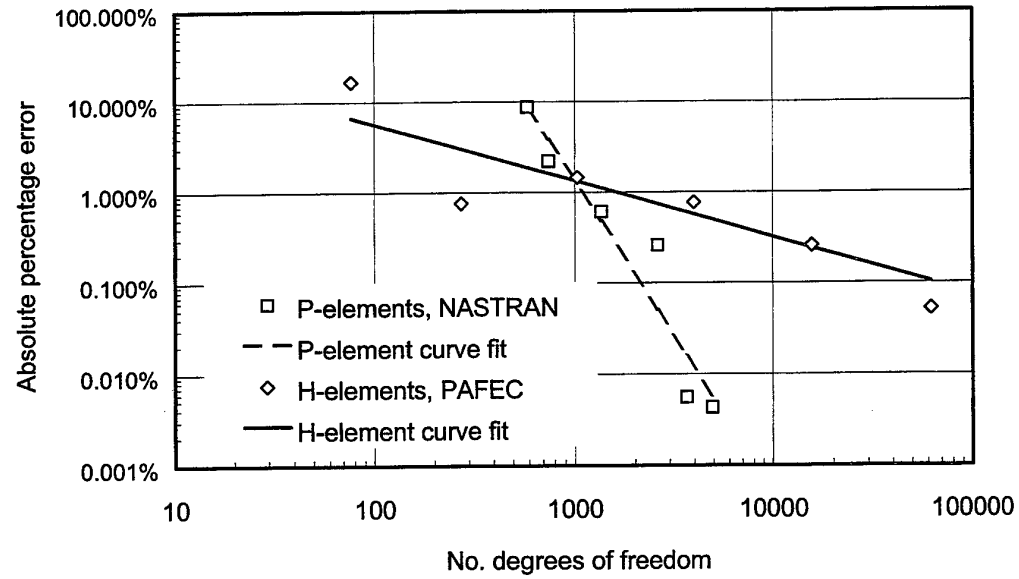

Figure 4: Relationship between absolute value of percentage error and degrees of freedom for 2D h- and p-element models.

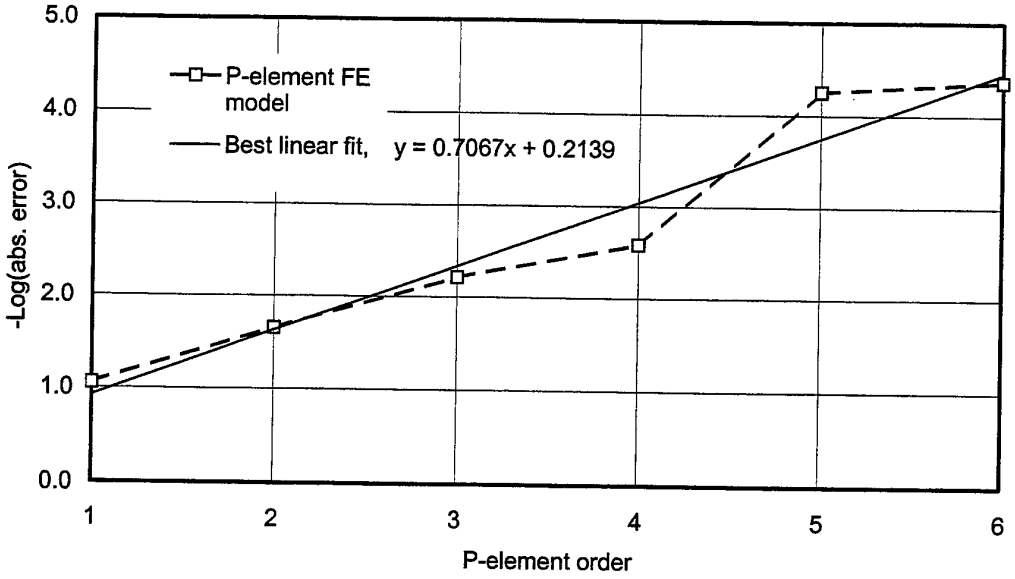

Figure 5: Relationship between log(abs. error) and p-element order for 2D models.

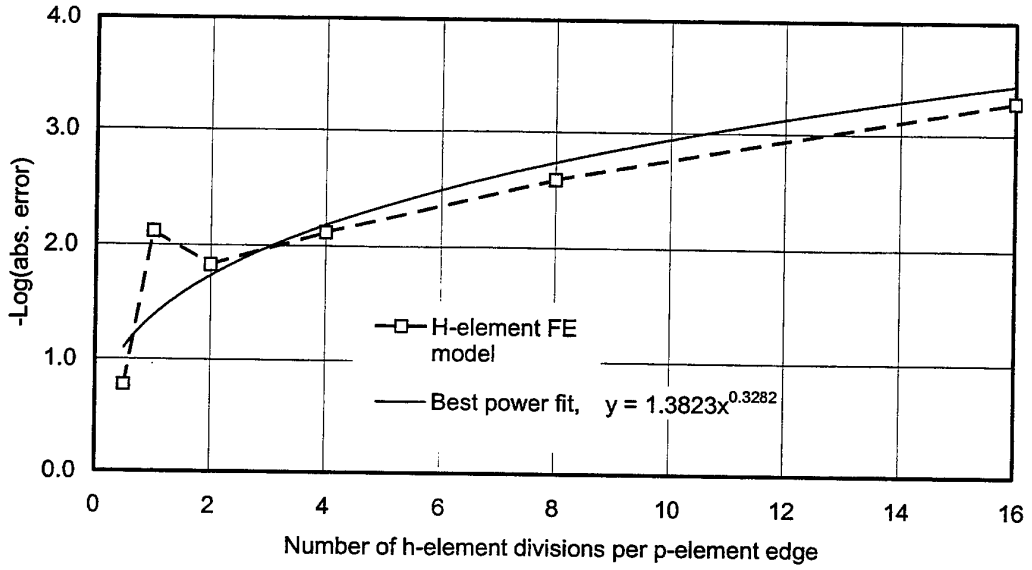

Figure 6: Relationship between log(abs. error) and h-element divisions for 2D models.

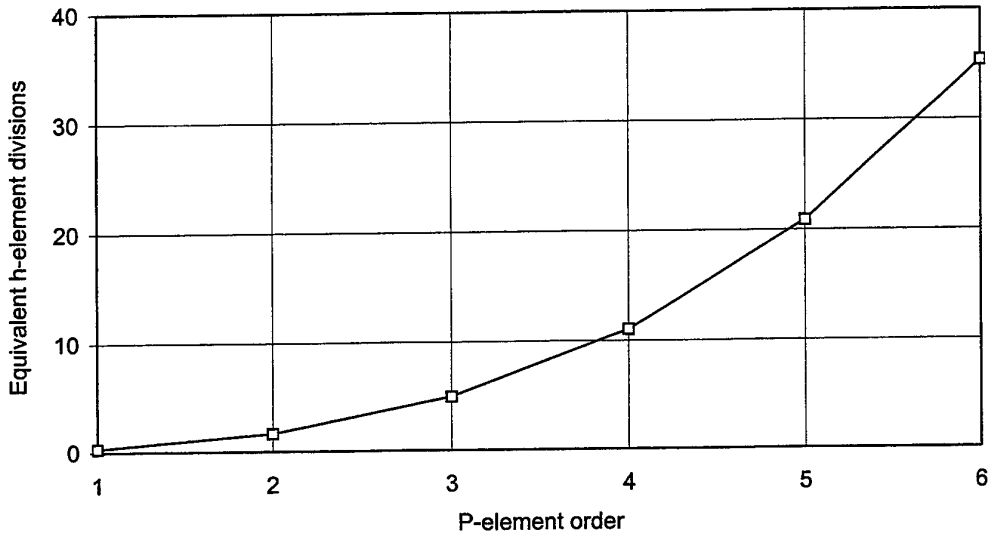

Figure 7: Relationship between p-element order and equivalent h-element divisions for 2D plate example.

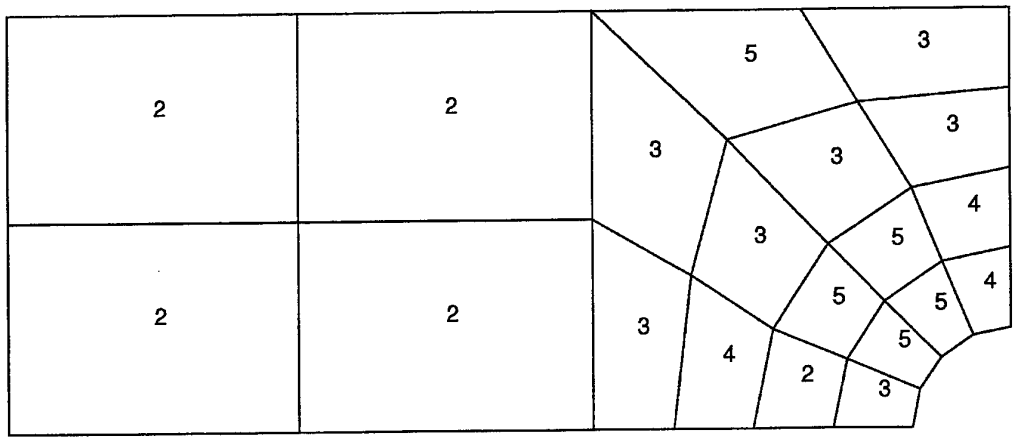

Figure 8: Distribution of final p-element orders from MSC.NASTRAN auto-order analysis.

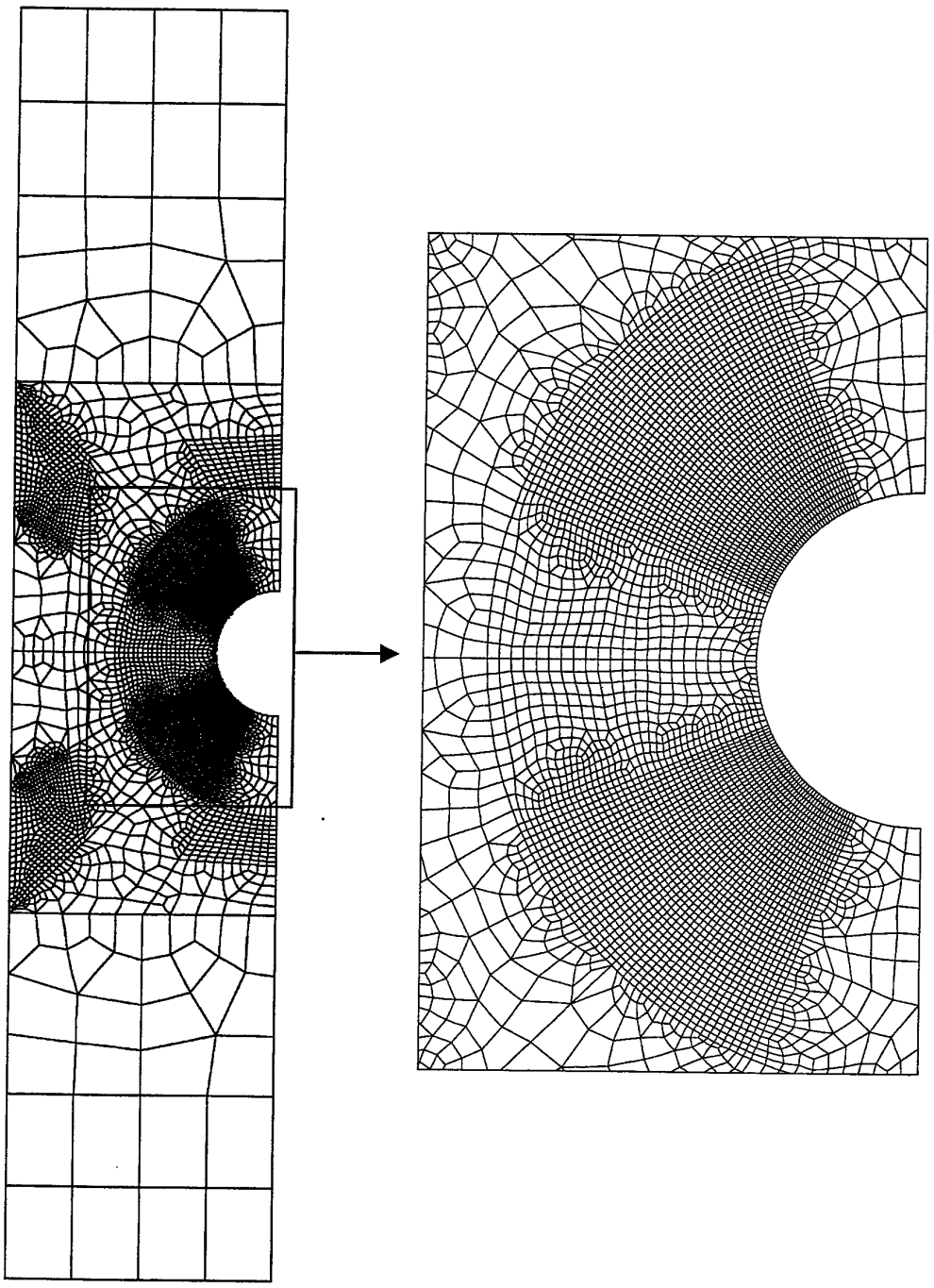

(a) Complete model *(b) Local detail near hole*

Figure 9: Two-dimensional h-element FE model based on empirical h-p relationship and final p-element orders.

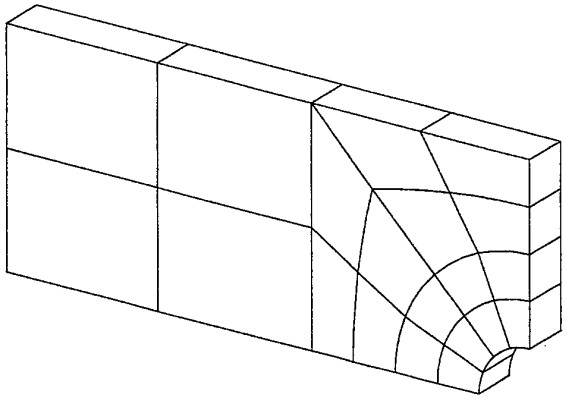

(a) One element through half thickness

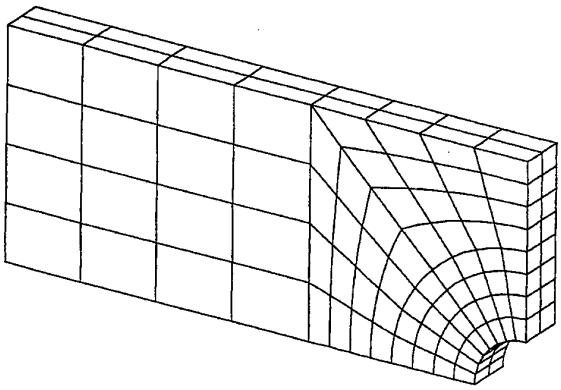

(b) Two elements through half thickness

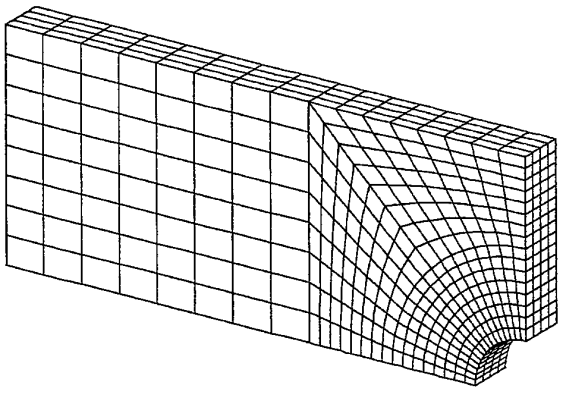

(c) Four elements through half thickness

Figure 10: Typical 3D finite element meshes for h-element analyses of plate specimen.

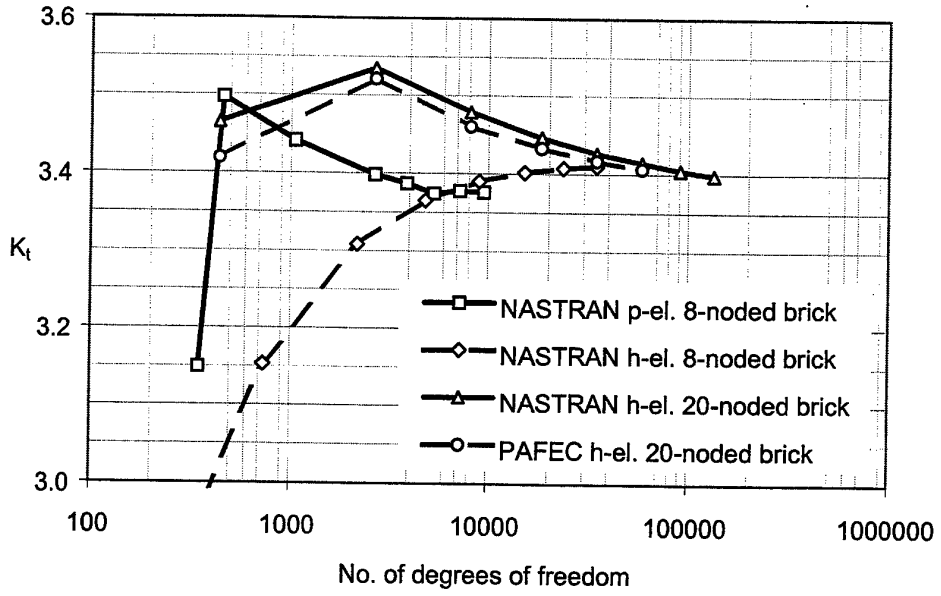

Figure 11: Variation of maximum stress concentration factor K_t with degrees of freedom for 3D h-element and p-element models.

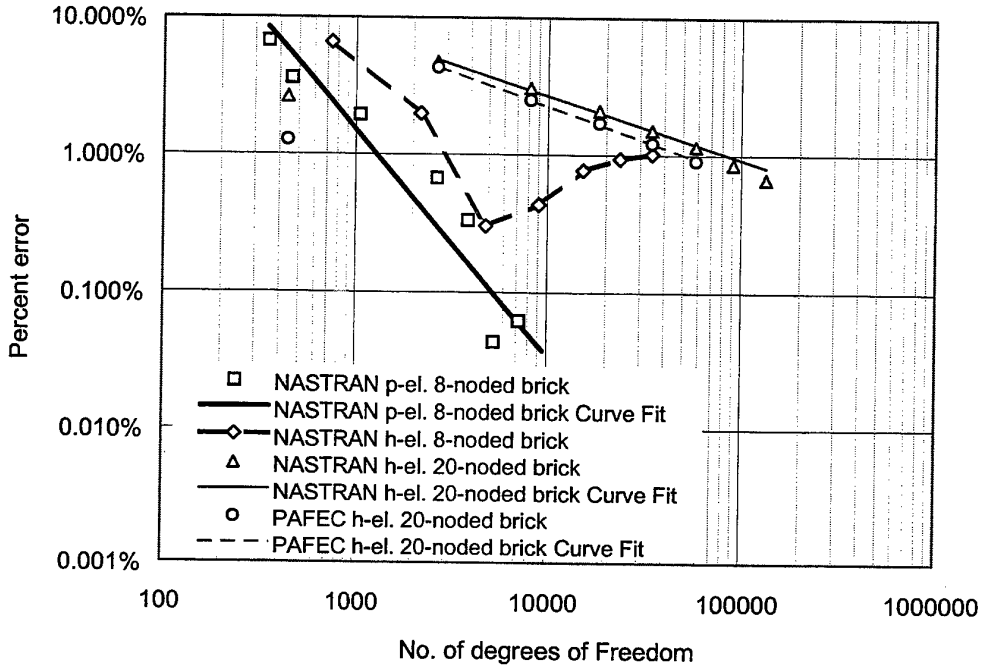

Figure 12: Variation of absolute percentage error with degrees of freedom for 3D h-element and p-element models.

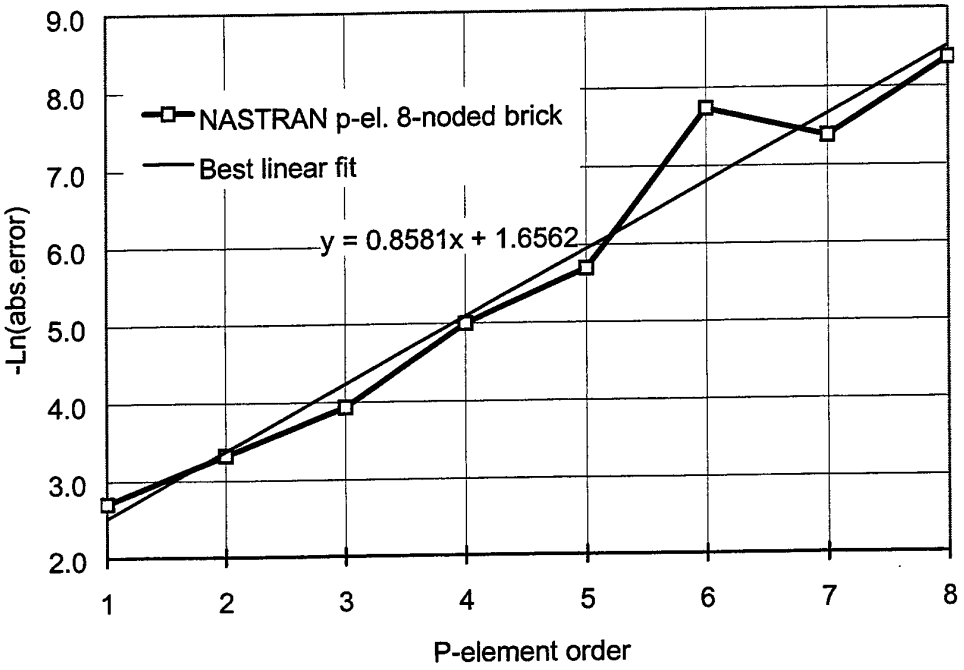

Figure 13: Relationship between ln(abs. error) and p-element order for 3D element models.

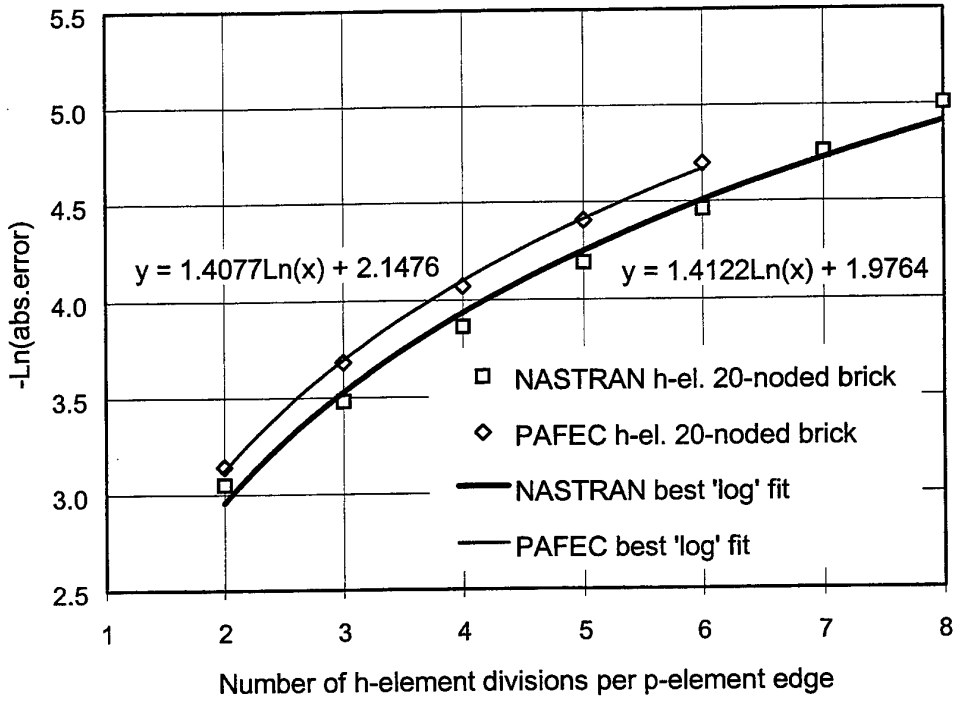

Figure 14: Relationship between ln(abs. error) and h-element divisions for 3D element models.

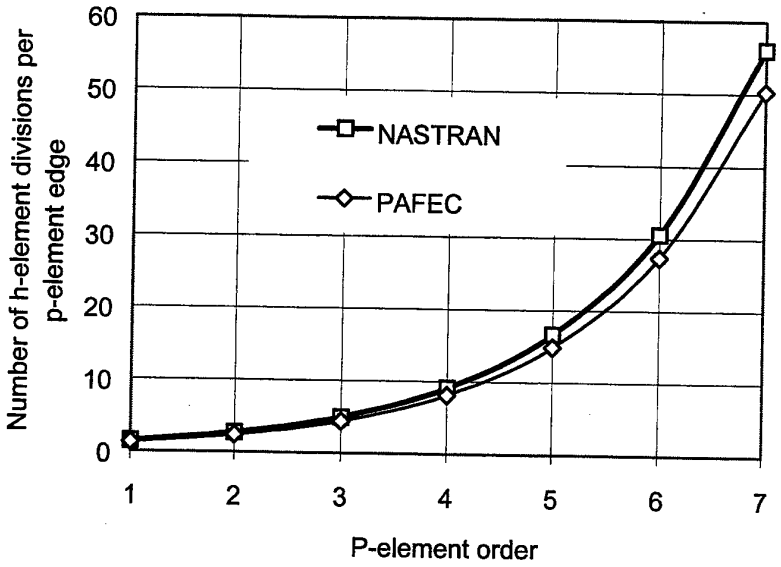

Figure 15: Relationship between p-element order and equivalent h-element divisions for 3D models.

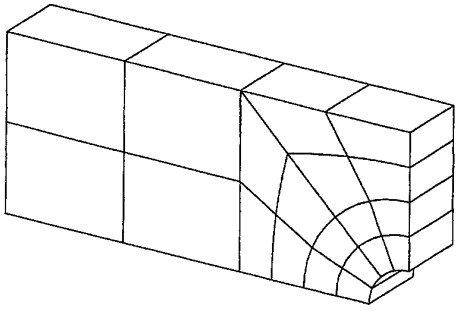

(a) One element through full thickness

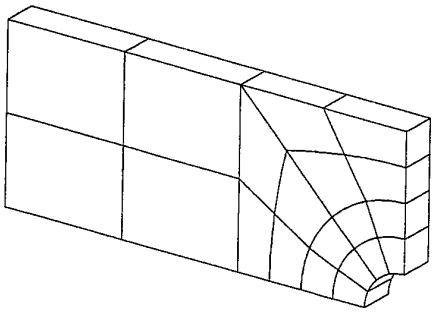

(b) One element through half thickness

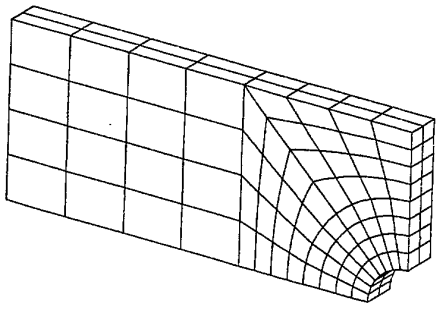

(c) Two elements through half thickness

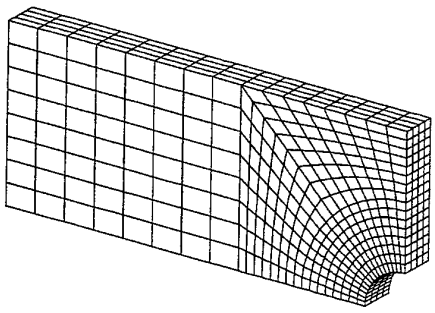

(d) Four elements through half thickness

Figure 16: P-element 3D FE models for through thickness stress analysis.

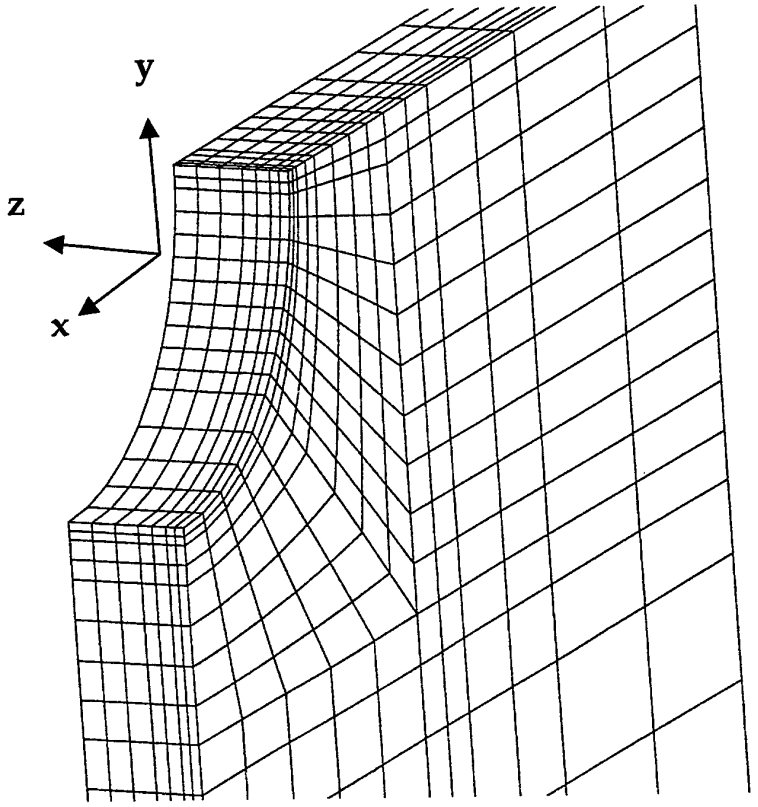

Figure 17: Local detail near hole for 3D finite element mesh used in prior PAFEC analysis [10].

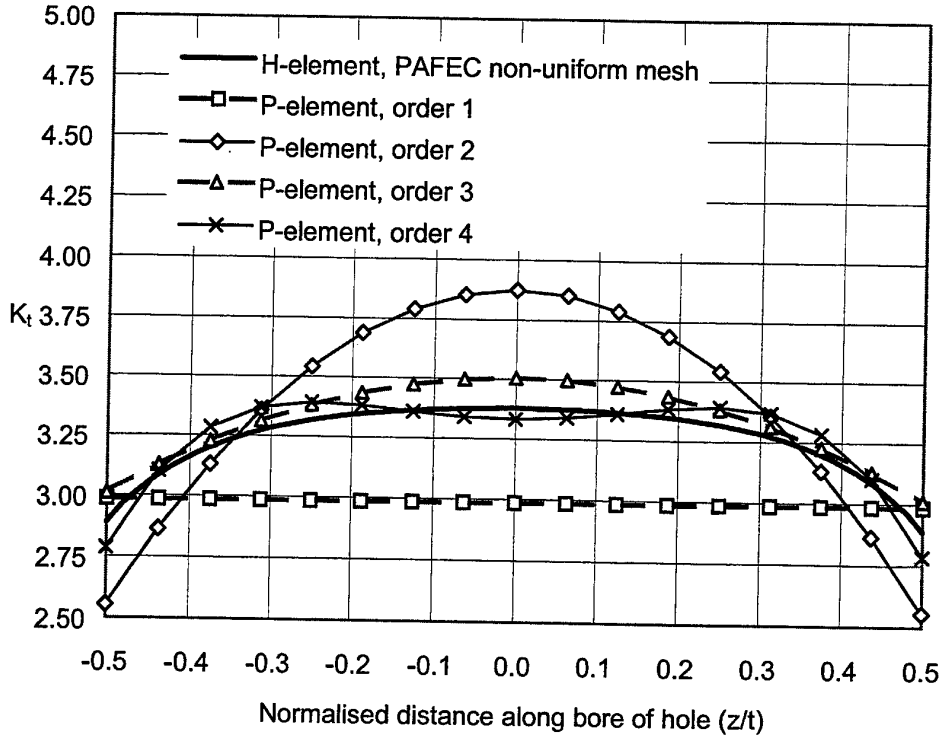

Figure 18: Stress concentration factor K_t along bore of hole for analysis with one element through full plate thickness and p-element orders 1 to 4.

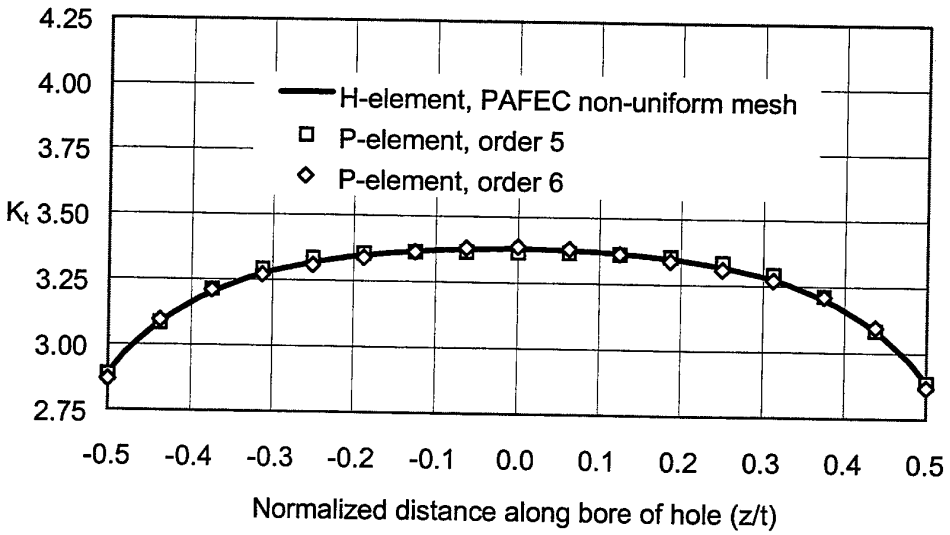

Figure 19: Stress concentration factor K_t along bore of hole for analysis with one element through full plate thickness and p-element orders 5 and 6.

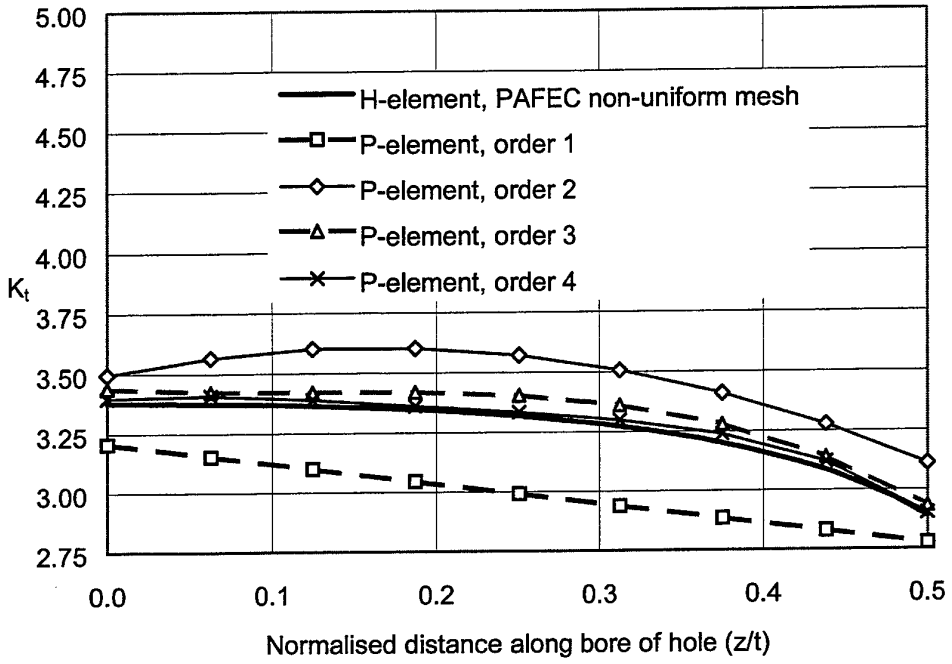

Figure 20: Stress concentration factor K_t along bore of hole for analysis with two elements through full plate thickness and p-element orders 1 to 4.

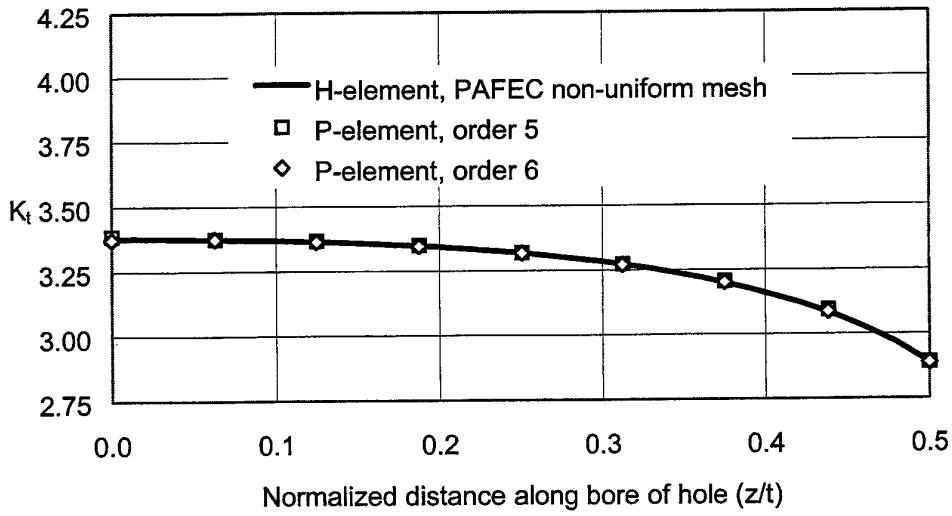

Figure 21: Stress concentration factor K_t along bore of hole for analysis with two elements through full plate thickness and p-element orders 5 and 6.

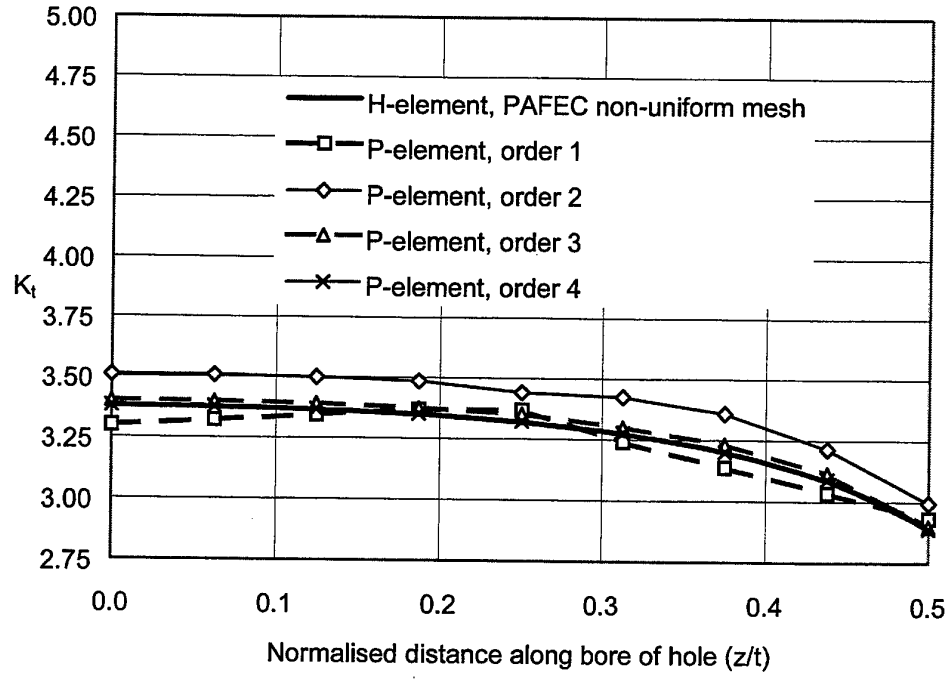

Figure 22: Stress concentration factor K_t along bore of hole for analysis with four elements through full plate thickness and p-element orders 1 to 4.

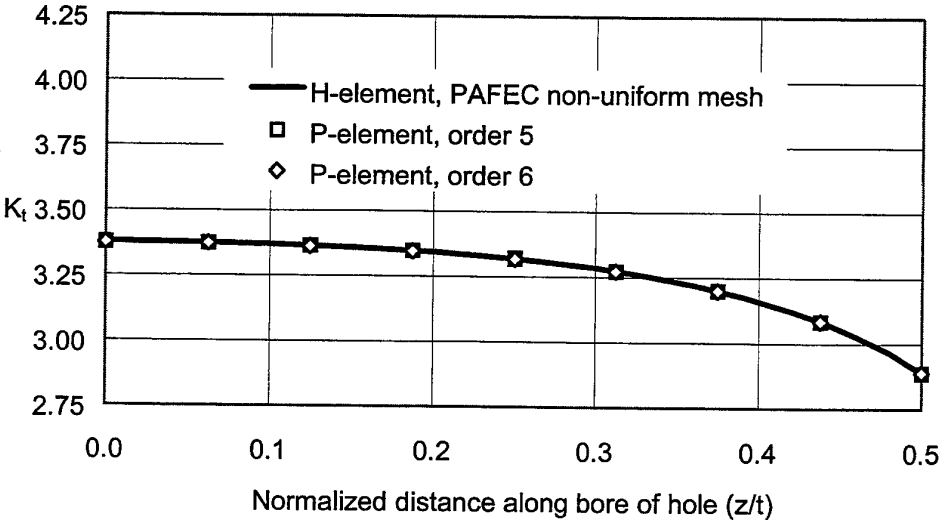

Figure 23: Stress concentration factor K_t along bore of hole for analysis with four elements through full plate thickness and p-element orders 5 and 6.

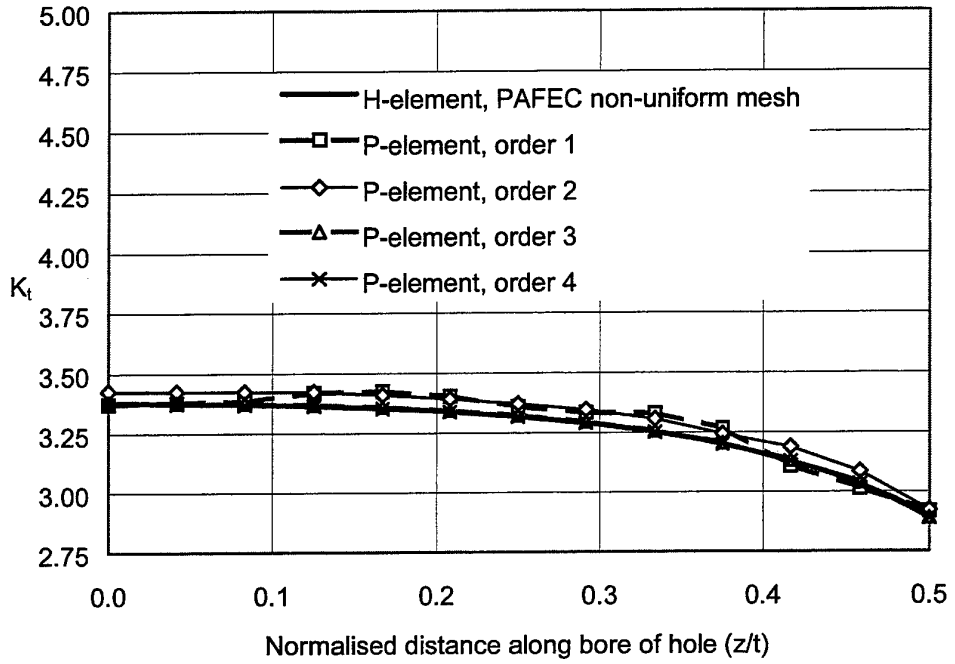

Figure 24: Stress concentration factor K_t along bore of hole for analysis with eight elements through full plate thickness and p-element orders 1 to 4.

DISTRIBUTION LIST

Notch Stress Convergence Studies for H and P Formulation Finite Elements

M.McDonald, M.Heller and R.J.Wescott

AUSTRALIA

DEFENCE ORGANISATION

Task Sponsor
RAAF DGTA

S&T Program
Chief Defence Scientist
FAS Science Policy
AS Science Corporate Management
Director General Science Policy Development
} shared copy
Counsellor Defence Science, London (Doc Data Sheet)
Counsellor Defence Science, Washington (Doc Data Sheet)
Scientific Adviser to MRDC Thailand (Doc Data Sheet)
Scientific Adviser Policy and Command
Navy Scientific Adviser (Doc Data Sheet and distribution list only)
Scientific Adviser - Army (Doc Data Sheet and distribution list only)
Air Force Scientific Adviser
Director Trials

Aeronautical and Maritime Research Laboratory
Director
Chief of Airframes and Engines Division
Research Leader Fracture Mechanics
Research Leader Aerospace Composite Structures
Research Leader Propulsion
Research Leader Structural Dynamics
Research Leader Structural Integrity
Authors: M.McDonald (7 copies)
M.Heller (10 copies)
R. Callinan
R. Chester
J. Hou
R. Kaye
S. Sanderson
W.Waldman
C. Wang
K. Watters
P. White
B. Wicks
A. Wong

DSTO Library and Archives

Library Fishermans Bend (Doc Data Sheet)
Library Maribyrnong (Doc Data Sheet)
Library Salisbury
Australian Archives
Library, MOD, Pyrmont (Doc Data sheet only)
US Defense Technical Information Center, 2 copies
UK Defence Research Information Centre, 2 copies
Canada Defence Scientific Information Service, 1 copy
NZ Defence Information Centre, 1 copy
National Library of Australia, 1 copy

Capability Systems Staff

Director General Maritime Development (Doc Data Sheet only)
Director General Aerospace Development

Knowledge Staff

Director General Command, Control, Communications and Computers (DGC4) (Doc Data Sheet only)
Director General Intelligence, Surveillance, Reconnaissance, and Electronic Warfare (DGISREW)R1-3-A142 CANBERRA ACT 2600 (Doc Data Sheet only)
Director General Defence Knowledge Improvement Team (DGDKNIT) R1-5-A165, CANBERRA ACT 2600 (Doc Data Sheet only)

Army

Stuart Schnaars, ABCA Standardisation Officer, Tobruck Barracks, Puckapunyal, 3662(4 copies)
SO (Science), Deployable Joint Force Headquarters (DJFHQ) (L), MILPO Gallipoli Barracks, Enoggera QLD 4052 (Doc Data Sheet only)
NPOC QWG Engineer NBCD Combat Development Wing, Tobruk Barracks, Puckapunyal, 3662 (Doc Data Sheet relating to NBCD matters only)

Intelligence Program

DGSTA Defence Intelligence Organisation
Manager, Information Centre, Defence Intelligence Organisation

Corporate Support Program

Library Manager, DLS-Canberra

UNIVERSITIES AND COLLEGES

Australian Defence Force Academy
Library
Head of Aerospace and Mechanical Engineering
Serials Section (M list), Deakin University Library, Geelong, 3217
Hargrave Library, Monash University (Doc Data Sheet only)
Librarian, Flinders University

OTHER ORGANISATIONS

NASA (Canberra)
AusInfo

Aerostructures Technologies
Author: R.J.Wescott (5 copies)

OUTSIDE AUSTRALIA

ABSTRACTING AND INFORMATION ORGANISATIONS

Library, Chemical Abstracts Reference Service
Engineering Societies Library, US
Materials Information, Cambridge Scientific Abstracts, US
Documents Librarian, The Center for Research Libraries, US

INFORMATION EXCHANGE AGREEMENT PARTNERS

Acquisitions Unit, Science Reference and Information Service, UK
Library - Exchange Desk, National Institute of Standards and Technology, US
National Aerospace Laboratory, Japan
National Aerospace Laboratory, Netherlands

SPARES (5 copies)

Total number of copies: **81**

DEFENCE SCIENCE AND TECHNOLOGY ORGANISATION
DOCUMENT CONTROL DATA

1. PRIVACY MARKING/CAVEAT (OF DOCUMENT)

2. TITLE

Notch Stress Convergence Studies for H and P Formulation Finite Elements

3. SECURITY CLASSIFICATION (FOR UNCLASSIFIED REPORTS THAT ARE LIMITED RELEASE USE (L) NEXT TO DOCUMENT CLASSIFICATION)

Document (U)
Title (U)
Abstract (U)

4. AUTHOR(S)

M.McDonald, M.Heller and R.J.Wescott

5. CORPORATE AUTHOR

Aeronautical and Maritime Research Laboratory
506 Lorimer St
Fishermans Bend Vic 3207 Australia

6a. DSTO NUMBER	6b. AR NUMBER	6c. TYPE OF REPORT	7. DOCUMENT DATE
DSTO-TR-1151	AR-011-864	Technical Report	May 2001

8. FILE NUMBER	9. TASK NUMBER	10. TASK SPONSOR	11. NO. OF PAGES	12. NO. OF REFERENCES
M1/9/846	AIR 98/220	RAAF DGTA	32	17

13. URL on the World Wide Web

http://www.dsto.defence.gov.au/corporate/reports/DSTO-TR-1151.pdf

14. RELEASE AUTHORITY

Chief, Airframes and Engines Division

15. SECONDARY RELEASE STATEMENT OF THIS DOCUMENT

Approved for public release

OVERSEAS ENQUIRIES OUTSIDE STATED LIMITATIONS SHOULD BE REFERRED THROUGH DOCUMENT EXCHANGE, PO BOX 1500, SALISBURY, SA 5108

16. DELIBERATE ANNOUNCEMENT

No Limitations

17. CASUAL ANNOUNCEMENT Yes

18. DEFTEST DESCRIPTORS

Stress intensity factors, Finite element analysis, Aircraft structures, Holes (openings), Mesh, Plates, Wing pivot fittings, F-111 aircraft

19. ABSTRACT

In the present investigation both 2D and 3D linear elastic analyses have been undertaken to assess the accuracy and computational resources associated with the use of h-element and p-element formulations. All analyses have been undertaken for a local stress-concentrating feature, which is typical of aircraft structures, namely a circular hole in a remotely loaded plate. Here highly accurate results are obtained for both element formulations, and it is found that the p-elements offer large savings in analysis times. Subsequently a relationship is developed and validated for both 2D and 3D meshes to determine an equivalent non-uniform h-element mesh density, which will yield the same accuracy as a fully converged p-element mesh. This provides a useful transferable tool for designing cost-effective h-element meshes, obviating the need for multiple mesh refinement iterations. Finally, it is demonstrated numerically that p-elements of order five and above, can be used to predict accurate through-thickness peak stresses, in a typical plate modelled with only one element through its full thickness.